
Maximal Domain Independent Representations Improve Transfer Learning

Adrian Shuai Li
 Purdue University
 West Lafayette, IN
 li3944@purdue.edu

Elisa Bertino
 Purdue University
 West Lafayette, IN
 bertino@purdue.edu

Xuan-Hong Dang
 IBM T. J. Watson Research Center
 Yorktown Heights, NY
 Xuan-Hong.Dang@ibm.com

Ankush Singla
 Purdue University
 West Lafayette, IN
 asingla@purdue.edu

Yuhai Tu
 IBM T. J. Watson Research Center
 Yorktown Heights, NY
 yuhai@us.ibm.com

Mark N Wegman
 IBM T. J. Watson Research Center
 Yorktown Heights, NY
 wegman@us.ibm.com

Abstract

Domain adaptation (DA) adapts a training dataset from a source domain for use in a learning task in a target domain in combination with data available at the target. One popular approach for DA is to create a domain-independent representation (DIRep) learned by a generator from all input samples and then train a classifier on top of it using all labeled samples. A domain discriminator is added to train the generator adversarially to exclude domain specific features from the DIRep. However, this approach tends to generate insufficient information for accurate classification learning. In this paper, we present a novel approach that integrates the adversarial model with a variational autoencoder. In addition to the DIRep, we introduce a domain-dependent representation (DDRep) such that information from both DIRep and DDRep is sufficient to reconstruct samples from both domains. We further penalize the size of the DDRep to drive as much information as possible to the DIRep, which maximizes the accuracy of the classifier in labeling samples in both domains. We empirically evaluate our model using synthetic datasets and demonstrate that spurious class-related features introduced in the source domain are successfully absorbed by the DDRep. This leaves a rich and clean DIRep for accurate transfer learning in the target domain. We further demonstrate its superior performance against other algorithms for a number of common image datasets. We also show we can take advantage of pretrained models.

1 Introduction

Labeling data for machine learning (ML) is a difficult and time-consuming process. In many instances, however, we may have labeled data similar to the data we are trying to label. For example, it is easier to label images presented in a familiar manner than labeling pictures taken with a color filter or an infrared camera. Therefore a question is whether it is possible to leverage existing labeled data to perform ML tasks like classification for similar data that is not labeled.

In this paper, we propose an approach to address such question based on transferring knowledge between related domains, referred to as domain adaptation (DA) [Zhang and Gao \[2022\]](#), [Zhang \[2021\]](#). In our setting, we have sufficient labeled data from a *source domain*. We are interested in assigning labels (from the set of labels in the source domain dataset) to data from a similar *target domain* with few or no labels. Examples of related domains are indoor vs outdoor pictures, summer vs winter pictures, or pictures with different resolutions. The source domain will generally have some information that is useful for labeling which is not available in the other domain. For instance, it is easier to identify ripe fruit in a low resolution color picture by using the color information. However, using the color information to classify grayscale pictures can lead to poor accuracy. Another general problem is that the characteristics of a domain may change over time. With older training samples, the test accuracy may deteriorate as the content of the domain evolves. DA uses information common to the different domains, hence it can be used for domains whose distribution changes over time.

One approach to achieve an effective DA is to generate a *domain-independent representation* (DIRep) of the data from different domains. A representation is domain independent if one cannot determine from the representation which domain the information came from. If based on the DIRep, we can classify the objects from the source domain, then there is a chance that we can classify the ones in the target domain as well. To generate a DIRep of the source and target data, one method is to adversarially train two neural networks, serving as a discriminator and generator, respectively.

However, the adversarial DA approach can suffer from what we call the *hidden data effect*. The hidden data effect can occur when the classifier can depend on shortcut information (spurious features) [Zewe \[2021\]](#) in the source domain that is not available in the target domain, and the shortcut information never the less persists into the DIRep. In the adversarial DA models, the generator's loss function trains the generator to maximize the accuracy of the classification on the source, which implies using the shortcut information, possibly in conjunction with other information in the source data. It also trains the generator so that its output is indistinguishable in both the source and target domains even though the input to the generator in the target does not have the shortcut information. The generator can resolve these conflicting goals, if with target data it creates pseudo-random shortcut information, with the same distribution as they occur in the source. This resolution requires that all DIRep information in the target that might not be consistent with the pseudo-random shortcut information be deleted from the output of the generator. This results in poorer performance of the classifier in the target domain because some of the information it needs would have been deleted.

To address the hidden data effect, we propose VAEGAN a new model that combines a variational autoencoder (VAE) with the GAN-based adversarial learning approach. In VAEGAN, we do classification based on the DIRep of the data. In order to achieve more accurate DA, the DIRep should contain as much information as possible. Reconstructing the input samples is a good measure to examine if VAEGAN can preserve all the information. However, without domain dependent information, reconstructing input samples solely from the DIRep is not possible. VAEGAN's solution to this problem is to encode all domain dependent information in a *domain-dependent representation* (DDRep). We thus add an autoencoder to our approach to ensure that the DIRep and the DDRep together contain enough information to reconstruct the input samples. To ensure that the DDRep only includes domain dependent information, we make it as small as possible (by using a VAE loss) without preventing reconstruction. The idea is that a maximal DIRep can be built by minimizing the DDRep.

The autoencoder forces most of the information needed for reconstruction into the DIRep, so the generator can no longer put shortcut based or, in the target case, pseudo random based results relevant to classification into the DIRep. They would now contradict the information needed to reconstruct the image. The information needed to reconstruct the image would include information that could be used to accurately classify and hence would contradict any pseudo random based results. That contradiction would enable the discriminator to recognize that the data came from the target. In this way we can at least partially defeat the hidden data effect.

We empirically test VAEGAN thoroughly and show that our model is both less vulnerable to the hidden data effect and outperforms other algorithms in unsupervised domain adaptation. VAEGAN works well when the weights of the generator are initialized to the value of some pre-trained model. In the experiments section we show that we can learn to classify even when the source domain has very little data, by initializing the generator with values that classify to categories that are not in the source or target domains.

2 Related Work

Transfer learning is an active research area that has been covered by several survey papers [Liu et al. \[2022\]](#), [Zhang and Gao \[2022\]](#), [Zhang \[2021\]](#), [Zhuang et al. \[2020\]](#), [Liu et al. \[2019\]](#), [Wang and Deng \[2018\]](#). These surveys categorize solutions into those relying on: data distribution discrepancy, pseudo-labeling, adversarial learning, reconstruction loss, and representation learning. Our solution falls in the intersection of adversarial learning, reconstruction loss and representation learning. We discuss the most relevant approaches in Sections 2.1 and 2.2.

2.1 Adversarial Learning based Approaches

These approaches typically aim at learning what we described as a DIRep by employing two competing networks of feature extractor/generator and domain discriminator. The domain adversarial neural network (DANN) [Ganin et al. \[2016\]](#), one of the first such approach, uses three network components, namely a feature extractor, a label predictor and a domain classifier. The generator is trained in an adversarial manner to maximize the loss of the domain classifier by reversing its gradients. The generator is trained at the same time as the label predictor to create a DIRep that contains domain-invariant features for classification. The adversarial discriminative domain adaptation (ADDA) [Tzeng et al. \[2017\]](#) approach adopts similar network components, yet its learning process involves multiple stages in training the three components of the model. Recently, the self-training guided adversarial domain adaptation (SGADA) [Akkaya et al. \[2021\]](#) method further extends ADDA by exploiting the performance of the discriminator in choosing relevant target samples to train the classifier. Singla et al. has proposed a hybrid version of the DANN and ADDA where the generator is trained with the standard GAN loss function [Goodfellow et al. \[2020\]](#). We refer to this as the GAN-based method [Singla et al. \[2020\]](#).

All adversarial learning based methods (DANN, ADDA, SGADA and GAN-based) aim at learning a common representation feature space between the source and target domains. They have all achieved similar results in classification in the target domain. However, depending on the details of the data and the networks, the DIRep may suffer from the aforementioned hidden data effect. Specifically, all these methods attempt to learn features that both fool the discriminator and lead an accurate classification for the source domain. Learning such features based purely on adversarial and supervised learning is challenging, since the features that can fool the discriminator might not lead to good classification results, and vice versa. As we show in our experiments, such hidden data effect can significantly degrade the classification performance in the target domain.

DANN and ADDA have recently been used based on pre-trained ResNet-50 models [Chen et al. \[2020\]](#).

2.2 Representation and Reconstruction based Approaches

A leading approach in this category is the Domain Separation Networks (DSN) [Bousmalis et al. \[2016\]](#). There are two extractors (generators) for each domain in DSN, one private and one shared, which create a private and a shared representation of the data corresponding to the DDRep and DIRep, respectively. The shared generator from the two domains is trained to produce a DIRep whose origins (source or target) cannot be determined. This shared generator hopefully captures the common features shared by the two domains. The shared and the private generators from each domain are trained to produce different results. Their DDRep and DIRep have the same shape, and they define a linear “soft subspace orthogonality constraint between the private and shared representation of each domain” to ensure that the DIRep and DDRep are as different as possible. The training of the shared generator in DSN is similar to the adversarial learning based approach. The new feature of DSN is the addition of a shared autoencoder that enforces the reconstruction of the data from the combined private and shared representations in each domain. At the same time, a classifier is trained from the shared representation (DIRep) of the source domain and the labels. Deep Reconstruction Classification Networks (DRCN) [Ghifary et al. \[2016\]](#) is another approach that relies on reconstruction to learn a common encoding representation shared between the two data domains.

By including an autoencoder, approaches like DSN require that all information needed for reconstruction is in either the DDRep or DIRep. We do so as well. This aids classification. We will show that DSN outperforms adversarial learning based methods such as DANN and GAN-based algorithms [Singla et al. \[2020\]](#).

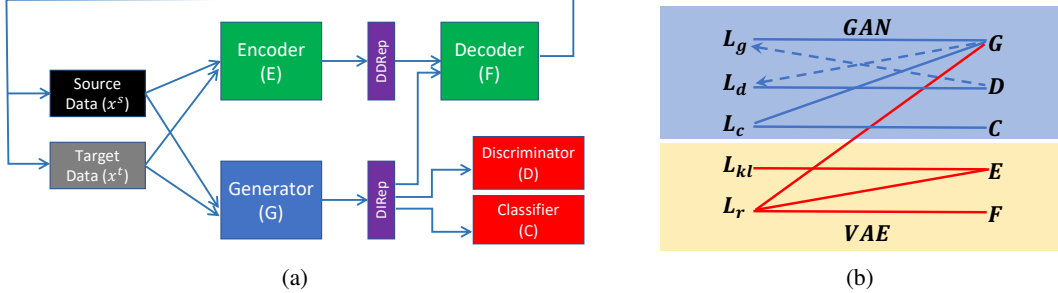


Figure 1: (a) Architecture of VAEGAN. (b) Illustration of the dependence between the loss functions and the neural networks (NN's) in the VAEGAN model. The only link between the GAN part of the model and the VAE part of the model is the dependence of \mathcal{L}_r on G . The dotted arrows represent one-sided dependence. For example, the dotted arrow from D to \mathcal{L}_g means that even though \mathcal{L}_g depends on D , the update of D only depends on the \mathcal{L}_d discriminator loss. All solid lines are bi-directions, i.e., the loss function depends on the NN and the updates of the NN depend on the loss function.

While DSN uses loss functions to ensure the DIRep and DDRep are linearly different, we use either loss functions or explicit construction to ensure that the DDRep contains as much information as possible. If the DSN does source classification when creating the DIRep, information needed for target classification may be found in the DDRep only via the hidden data effect. Moreover, the linear orthogonality may not guarantee a strict distinction between DIRep and DDRep, as the same (original) information can still be encoded into both of them in a non-linear manner. Furthermore, if a feature is encoded in the DDRep early in training, this may prevent it from being used for classification later, as the DIRep is required to be orthogonal to the DDRep. All these shortcomings of DSN can lead to some degree of hidden data effect, which can potentially lower the classification accuracy in the target domain. Our approach aims to improve domain adaptation performance by reducing/eliminating some of these shortcomings.

3 The VAEGAN for Domain Adaptation

In this section we formulate our model that combines GAN-based DA with a variational autoencoder (VAE) to create a maximal DIRep for transfer learning. Fig. 1(a) shows the architecture of our model, referred to as VAEGAN.

(1) Networks. There are five neural networks (by neural network, we mean the network architecture and all its weights) in the algorithm: 1) G is the generator; 2) D is the discriminator; 3) C is the classifier; 4) E is the encoder; 5) F is the decoder.

(2) Inputs and outputs. The data is given by (x, l, d) where x is the input; we use the notation x^s and x^t to respectively represent the source and target data samples, when necessary to distinguish them. l is the label of sample x (if any), and d is the domain identity (e.g., can be as simple as one bit of 0 for the source domain and 1 for the target domain). In the zero-shot or few-shot domain adaptation settings, l is available for all source data samples, but none or only a few are known for the target samples. x is the input given to both encoder E and generator G . The DDRep and DIRep correspond to the intermediate outputs of E and G , respectively:

$$DDRep = E(x), \quad DIRep = G(x), \quad (1)$$

which then serve as the inputs for the downstream networks F , D , and C . In particular, DIRep serves as the input for D and C , and both DIRep and DDRep serve as the inputs for F . The outputs of these three downstream networks are \hat{x} from the decoder F ; \hat{d} from the discriminator D ; and \hat{l} from the classifier C . These outputs are:

$$\hat{x} = F(DDRep, DIRep) = F(G(x), E(x)), \quad (2)$$

$$\hat{d} = D(DIRep) = D(G(x)), \quad (3)$$

$$\hat{l} = C(DIRep) = C(G(x)), \quad (4)$$

where we list the dependence of the outputs on the corresponding networks explicitly.

(3) Loss functions. Some measures of the differences between the predictions from the networks, i.e., $(\hat{x}, \hat{d}, \hat{l})$ and their actual values (x, d, l) are used to construct the loss functions. Typically a loss function would take two arguments, a prediction and the actual label/value. We often use the name of the loss function without specifying the arguments, and do so for the discriminator, generator, classification and reconstruction losses. Like a variational autoencoder (VAE), we introduce an additional KL divergence loss function for E to create a minimal DDRep so we can force most of the input information into the DIRep. All the loss functions with their dependence on specific neural networks are given explicitly here: (1) Classification loss: $\mathcal{L}_c = \mathcal{L}_c(\hat{l}, l) = \mathcal{L}_c(C(G(x), l))$. (2) Discriminator loss: $\mathcal{L}_d = \mathcal{L}_d(\hat{d}, d) = \mathcal{L}_d(D(G(x), d))$. (3) For the generator loss, we want to train the generator to fool the discriminator. So, the generator has a smaller loss when the discriminator makes the wrong prediction: $\mathcal{L}_g = \mathcal{L}_g(\hat{d}, 1 - d) = \mathcal{L}_d(D(G(x)), 1 - d)$. (4) Reconstruction loss: $\mathcal{L}_r = \mathcal{L}_r(\hat{x}, x) = \mathcal{L}_r(F(G(x), E(x)), x)$. (5) KL loss for DDRep: $\mathcal{L}_{kl} = D_{KL}(Pr(E(x)) \parallel \mathcal{N}(0, I))$. For the reconstruction loss \mathcal{L}_r , we used the L_2 -norm. For $\mathcal{L}_d, \mathcal{L}_g, \mathcal{L}_c$, we used cross entropy. More details can be found in Appendix A. The dependence of the loss functions on the neural networks in the VAEGAN algorithm is shown in Fig.1(b).

(4) The back-prop based learning. The gradient-descent based learning dynamics for updating the five neural networks is described by the following equations:

$$\begin{aligned} \Delta G &= -\alpha_G \left(\lambda \frac{\partial \mathcal{L}_g}{\partial G} + \beta \frac{\partial \mathcal{L}_c}{\partial G} + \gamma \frac{\partial \mathcal{L}_r}{\partial G} \right), & \Delta E &= -\alpha_E \left(\frac{\partial \mathcal{L}_{kl}}{\partial E} + \mu \frac{\partial \mathcal{L}_r}{\partial E} \right), \\ \Delta C &= -\alpha_C \frac{\partial \mathcal{L}_c}{\partial C}, & \Delta D &= -\alpha_D \frac{\partial \mathcal{L}_d}{\partial D}, & \Delta F &= -\alpha_F \frac{\partial \mathcal{L}_r}{\partial F}, \end{aligned}$$

where $\alpha_{C,D,E,F,G}$ are the learning rates for different neural networks. In our experiments, we often set them to the same value, but they can be different in principle. The other hyperparameters λ, β, γ , and μ are the relative weights of the loss functions. These hyperparameters are also useful to understand the different algorithms. In fact, $\gamma = 0$ corresponds to the GAN-based algorithm presented in [Singla et al. \[2020\]](#). As easily seen from the equations above, when $\gamma = 0$, the GAN-based algorithm (blue/upper part in Fig.1(b)) decouples from the VAE based constraints (yellow/lower part in Fig.1(b)).

3.1 The Explicit DDRep Algorithm

To make the DIRep contain as much information as possible, we introduce a simplified *explicit DDRep algorithm* without the encoder E and set the DDRep explicitly to be the domain label (bit) d , i.e., $DDRep = d$. A variant of this approach is to add d to the DDRep generated by the encoder. d is the simplest possible domain dependent information that could serve to filter out the domain dependent information from the DIRep.

We were surprised that in several cases the explicit DDRep performs as well as the VAEGAN. We think the VAEGAN is more general, which is why we focus on it. When doing experiments with the VAEGAN model we observed that the KL divergence of the DDRep corresponds to less than one bit measured as entropy. What we believe happens is that the DIRep contains information to describe both the original data and some generated information describing an alternative as if it came from the other domain. Then the DDRep merely has enough information for the decoder to determine which information to use in reconstructing the original data.

One useful feature of this simplified algorithm is that it allows us to check the effect of the DDRep directly by flipping the domain bit ($d \rightarrow 1 - d$). We know the domain bit is effective in filtering out domain dependent information from the DIRep if the reconstructed image $\hat{x} = F(DIRep, 1 - d)$ resembles an image from the other domain as shown in Fig.2.

3.2 Comparing VAEGAN to DSN

Our VAEGAN model shares several features with DSN. However, it does not limit DDRep and DIRep to be in the same embedding space, giving them freedom to capture different features from source and target samples. Moreover, VAEGAN goes beyond the *linear* orthogonality by exploiting the *non-linear* KL-divergence in much the same way the conventional VAEs work. Specifically, our

VAEGAN attempts to keep DDRep as small as possible. As demonstrated in one set of our experiments on the Fashion-MNIST, the DDRep can be as small as a single bit, yet it still gets the task done properly. The advantage of keeping DDRep small is that VAEGAN can force as much common sharing information between the two domains as possible into the DIREp, which maximizes the chances of success for the classifier C in both data domains.

4 Experiments

We now evaluate VAEGAN across different adaptation settings. We first demonstrate that in an artificial setting the hidden data effect takes place. Then we consider a more natural settings to show that we have a real advantage over a DANN like system and even a DSN like system. Since the generator and classifier topologies are the same in all of these systems, we need to show that the weights trained by VAEGAN are usually better. The DANN systems may occasionally have the same performance as VAEGAN. Thus we have used multiple runs and a z-score to assess whether one set of runs is statistically better than another.

Cheating is our technique for encouraging the hidden data effect. If you do a Google search for images of wolves, probably half of them are in snow. If you do a Google search for dogs, none of them are likely to be in snow. So if we want to classify dogs from wolves where the domain is images on the internet, snow is very helpful. But suppose you want to classify dogs from wolves in the results stemming from the query “animals in winter”. In that case, snow is useless. By adding information to enable a classifier of images to “cheat” by using useful information only available in one domain, we have found we encourage the hidden data effect. What we call cheating is a common problem that occurs in some natural DAs.

We construct several DA scenarios where some cheating clue exist in the source domain based on two widely used image datasets: (1) Fashion-MNIST¹, which consists of 60,000 grayscale images for training and 10,000 images for testing. Each image is represented as a 2-dimensional tensor of 28×28 and belongs to one of 10 classes; (2) CIFAR-10 dataset² which consists of 50,000 images for training and 10,000 images for testing from 10 classes. Each image is represented by a $32 \times 32 \times 3$ tensor (i.e., a color image with 3 channels of Red, Green and Blue).

We also validate our model on the standard benchmarks for unsupervised DA. We assessed three different adaptation scenarios by using four digits datasets, namely MNIST [LeCun et al. \[1998\]](#), MNIST-M [Ganin et al. \[2016\]](#), Street View House Number [Netzer et al. \[2011\]](#) and synthetic digits [Ganin et al. \[2016\]](#). Finally, we evaluate on the Office [Saenko et al. \[2010\]](#) dataset for comparison against other unsupervised DA approaches.

4.1 Benchmarks that demonstrate hidden data effect

4.1.1 Fashion-MNIST Classification

Fashion-MNIST is a well known dataset, which we use as a source domain. We construct a target domain by flipping the images of 180° . To simulate shortcut information, we add to the source data set a one hot vector that contains the correct classification. We call that information cheating bits, because it is not available in the target domain. To the target dataset we also add some bits, but they either include information suggesting a random classification (random cheating), so the shortcut information is useless in the target domain or one that is shifted to the next label from the correct label (shift cheating), so it is always wrong, but perhaps in a predictable way. The one-hot bits have the same distribution in the source and target data sets, so if they are reflected in the DIREp the discriminator would not detect the difference between source and target. In this case, a classifier learned from this partial representation would perform poorly on the target data.

Benchmark algorithms. We compare our method against the prevailing unsupervised DA approaches: GAN-based approach [Singla et al. \[2020\]](#), Domain-Adversarial Neural networks (DANN) [Ganin et al. \[2016\]](#) and Domain Separation Networks (DSN) [Bousmalis et al. \[2016\]](#). We implemented both VAEGAN and the explicit DDRep algorithm in the zero-shot setting. We only report

¹<https://github.com/zalandoresearch/fashion-mnist>

²<https://www.cs.toronto.edu/~kriz/cifar.html>

Table 1: Mean classification accuracy (%) of different unsupervised DA approaches for the constructed Fashion-MNIST datasets.

| Model | No cheating | Shift cheating | Random cheating |
|-------------|-------------|----------------|-----------------|
| Source-only | 20.0 | 11.7 | 13.8 |
| GAN-based | 64.7 | 58.2 | 54.8 |
| DANN | 63.7 | 58.0 | 53.6 |
| DSN | 66.8 | 63.6 | 57.1 |
| VAEGAN | 66.9 | 65.7 | 61.6 |
| Target-only | 88.1 | 99.8 | 87.9 |

Table 2: z-test score value comparing VAEGAN to other models for constructed Fashion-MNIST. $z > 2.3$ means the probability of VAEGAN being no better is ≤ 0.01 .

| Model | No cheating | Shift cheating | Random cheating |
|-----------|-------------|----------------|-----------------|
| GAN-based | 1.55 | 3.28 | 3.68 |
| DANN | 2.26 | 4.17 | 4.33 |
| DSN | 0.16 | 2.60 | 3.18 |

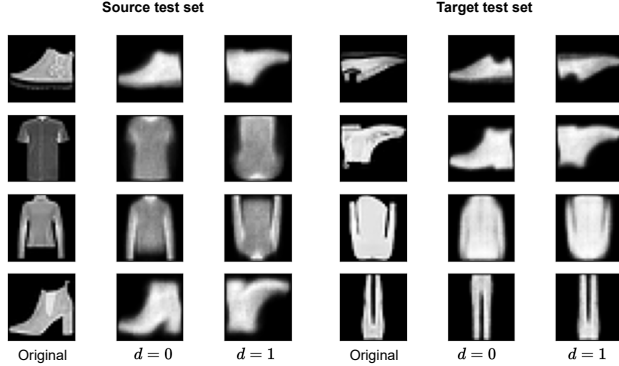


Figure 2: Columns 1 and 4, original images; 2 and 6, reconstructions of originals; 3 and 5, reconstructions with domain bit flipped.

the results about the explicit DDRep algorithm as it achieves almost identical performance on this task. We also provide two baselines, a classifier trained on the source domain samples without DA (which gives us the lower bound on target classification accuracy) and a classifier trained on the target domain samples (which gives us the upper bound on target classification accuracy). We compare our ability to ignore the cheating bits in Table 1 and Table 2. More details of the topology, learning rate, hyper-parameters setup and results analysis is provided in Appendix B.

As we mentioned, the decoder learns to reconstruct the image by using DIRep and DDRep (domain bit) together. Figure 2 shows reconstructed images for the shift cheating scenario. The reconstructed images are a bit fuzzier and perhaps a bit more like generic images of elements in the same class. Some details seem to be getting lost despite the reconstruction. Nevertheless, the reconstructed images have rendered the domain bit effective in filtering out domain-dependent information, as the reconstructed images look like they are from the other domain when we flip the domain bit.

4.1.2 CIFAR-10 Classification

We are interested in more natural DA scenarios where the source and target images might be captured with different sensors and thus have different wavelengths and colors. To address this use case, we created our source and target datasets based on CIFAR-10³ with different color planes. Furthermore, we introduced the cheating color plane where the choice of the color planes in the source data have some spurious correlation with the labels. We observe similar hidden data effect on the CIFAR-10 set with spurious correlation, suggesting that the optimization difficulties of previous methods and the results of our methods are not limited to a particular dataset.

The source set with cheating color planes is constructed as follows. First, we encode labels in CIFAR-10 with values between 0 and 9. Then for each CIFAR-10 image, if its label is odd, we keep only the B channel with prob p , and randomly keep the B or the R channel for the rest. Similarly, if the label is even, with prob p , the image has only the R color channel, and either the R or B channel is kept for the rest. For example, when $p = 1$, all images with odd labels have only the B channel and all images with even labels have only the R channel. We call p the *bias* since it controls the strength of the spurious correlation between the color of the image and its label. In the target domain, for

³<https://www.cs.toronto.edu/~kriz/cifar.html>

Table 3: Averaged classification accuracy (%) of different unsupervised DA approaches for constructed CIFAR-10 dataset with a spectrum of bias.

| Model | 0% bias | 20% bias | 40% bias | 60% bias | 80% bias | 90% bias | 100% bias |
|-------------|-------------|-------------|-------------|-------------|-------------|-------------|-------------|
| Source-only | 10.0 | 10.0 | 10.0 | 10.0 | 10.0 | 10.0 | 10.0 |
| GAN-based | 63.0 | 62.5 | 61.4 | 56.9 | 53.2 | 44.5 | 30.1 |
| DANN | 62.7 | 62.0 | 61.0 | 56.5 | 52.2 | 42.9 | 29.1 |
| DSN | 68.7 | 67.9 | 67.3 | 67.5 | 64.5 | 61.7 | 32.2 |
| VAEGAN | 70.4 | 69.8 | 69.8 | 69.7 | 68.2 | 64.1 | 34.2 |
| Target-only | 78.9 | 78.9 | 78.9 | 78.9 | 78.9 | 78.9 | 78.9 |

Table 4: z-test score value comparing VAEGAN to other models for constructed CIFAR-10. $z > 2.3$ means the probability of VAEGAN being no better than the other models is ≤ 0.01 .

| Model | 0% bias | 20% bias | 40% bias | 60% bias | 80% bias | 90% bias | 100% bias |
|-----------|---------|----------|----------|----------|----------|----------|-----------|
| GAN-based | 5.23 | 3.20 | 5.93 | 12.8 | 11.31 | 7.20 | 4.58 |
| DANN | 5.44 | 3.42 | 6.22 | 13.2 | 12.02 | 7.79 | 5.70 |
| DSN | 2.68 | 3.00 | 3.95 | 3.47 | 7.43 | 3.78 | 2.23 |

each CIFAR-10 image we keep only the G channel regardless of the label. We compare our approach and the others with p taking values from the set $\{0, 0.2, 0.4, 0.6, 0.8, 0.9, 1.0\}$. A larger value of p indicates a higher level of spurious correlation in the source data and thus a more challenging DA task.

In this ‘‘cheating-color-plane’’ setting, the GAN-like algorithms might cheat by leveraging the correlation between the presence or absence of the color planes and the label of the image to create an easier classification scheme for the labeled source data. Consequently, the DIRep would include false cheating clues which can degrade performance for the target data where the cheating clues lead to the wrong answer.

We report the mean accuracy of different unsupervised DA methods and our approach on the target test set in Table 3. The z-scores of comparing our method with other methods are shown in Table 4. The details of the experiment and analysis of the results are included in Appendix C.

4.1.3 Semi-supervised Domain Adaptation

As an additional experiment, we also evaluated the proposed algorithm for semi-supervised DA on the constructed CIFAR-10 datasets. The model is provided with a majority of unlabeled target data and a small amount of labeled target data. In our setting, we revealed 1, 5, 10, 20, 50 and 100 samples per class which we then used for contributing to the classification loss through the label prediction pipeline. We also provided the same number of labels for the GAN and DSN method. We skipped the DANN method since its performance is very similar to the GAN approach. More importantly, we ask the following question: *How much does each algorithm gain from a small labeled target training set for different biases?* The classification loss on the target ensures that the generator does not get away with learning a DIRep that contains only the cheating clue, which could bias the model during training and cause a high classification loss.

We select four most representative biases and show the results in Figure 3. For 40%, 60% and 80% biases, the classification accuracy does improve, but not significantly as the number of target labels increases. The performance order of VAEGAN > DSN > GAN-based is preserved. When the bias is equal to 100%, the performance curves are quite different. All of them increase significantly with the number of target labels, while the order of performance is preserved. While all three algorithms benefit from a small number of target labeled samples, VAEGAN improves the most, surpassing DSN and GAN-based results by 12% and 25% respectively with only a total of 50 target labels (note that it corresponds to 5 labels/class in Figure 3).

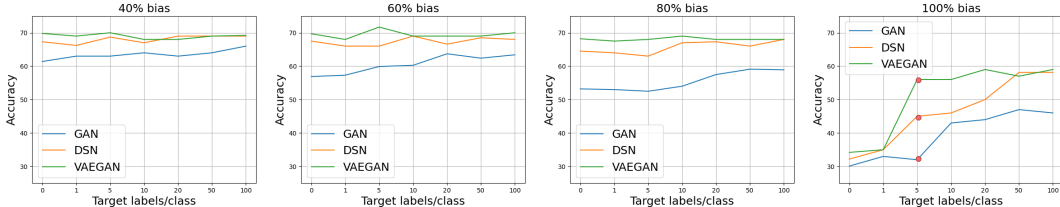


Figure 3: Mean classification accuracy on CIFAR-10 with semi-supervised setting for three different unsupervised DA algorithms. Overall, a few target labels improve classification accuracy. The improvement is significant in 100% bias setting.

Table 5: Mean classification accuracy (%) of different unsupervised domain adaptation approaches for widely used benchmarks. The results are cited from each study.

| Model | MNIST to MNIST-M | Synth Digits to SVHN | SVHN to MNIST |
|-------------|------------------|----------------------|---------------|
| Source-only | 56.6 | 86.7 | 59.2 |
| DANN | 76.6 | 91.0 | 73.8 |
| DSN | 83.2 | 91.2 | 82.7 |
| VAEGAN | 81.0 | 91.1 | 85.8 |
| Target-only | 98.7 | 92.4 | 99.5 |

Table 6: Mean classification accuracy (%) of different unsupervised domain adaptation approaches for the office dataset. We have cited the original results (if applicable) and in parentheses we show the results reported in Chen et al. [2020] with data augmentation.

| Model | $A \rightarrow W$ | $D \rightarrow A$ | $W \rightarrow A$ |
|-------------|----------------------|-------------------|-------------------|
| Source-only | 64.2 (68.4) | - (62.5) | - (60.7) |
| DANN | 73.0 (82.0) | - (68.2) | - (67.4) |
| ADDA | 75.1 (86.2) | - (69.5) | - (68.9) |
| VAEGAN | 82.0 | 72.9 | 72.0 |

4.2 Standard DA benchmarks

4.2.1 Digits datasets

In this experiment, we use three unsupervised domain adaptation pairs: 1) MNIST \rightarrow MNIST-M, 2) Synth Digits \rightarrow SVHN, and 3) SVHN \rightarrow MNIST. Example images from all four datasets are provided in Figure 5 of Appendix D. The architecture and hyper-parameter settings are provided in Appendix D due to a limit of space.

Table 5 shows the results on the digits datasets. We cited the results from each study to make a fair comparison. In MNIST \rightarrow MNIST-M and Synth Digits \rightarrow SVHN, we were not able to achieve the published results for DSN. The previously published results for DSN were based on using hyperparameters chosen after using 1000 labeled samples from the target. Our parameters were chosen without use of target labels. In summary, VAEGAN outperforms DSN on SVHN \rightarrow MNIST and is at least comparable elsewhere.

4.2.2 Office datasets

The Office dataset has 4110 images from 31 classes in three domains: amazon (2817 images), webcam (795 images) and dslr (498 images). The three most challenging domain shifts reported in previous works are amazon to webcam ($A \rightarrow W$), dslr to amazon ($D \rightarrow A$) and webcam to amazon ($W \rightarrow A$). In $D \rightarrow A$ and $W \rightarrow A$ are the cases with the least labelled information.

We follow the previous work in Tzeng et al. [2017], Chen et al. [2020] which use a pretrained ResNet-50 on ImageNet Deng et al. [2009] as a base. Details are provided in the Appendix E. We present the results in Table 6. We include the original results from the DANN and ADDA papers as well as the new results from Chen et al. [2020] with training data augmentation. VAEGAN is competitive on this adaptation task, matching the performance of DANN and outperforming the other approaches in $D \rightarrow A$ and $W \rightarrow A$ without using any data augmentation.

5 Conclusion and Future Work

In this paper, we have described the challenges in DA caused by the hidden data effect and presented a better solution than previous methods for a number of common image datasets. The hidden data effect is more likely to appear in more complex data problems, e.g., we see more of its impact in CIFAR than in Fashion-MNIST. The hidden data effect is also likely to appear when there is a drift in data, making classification more difficult. We showed that using a DIRep and DDRep trained with both a variational autoencoder and a discriminator makes a good base (DIRep) for a classifier, when

we add pressure for the DDRep to be small. It would be interesting to test our method in these more complex problems.

In the case where there is a limited number of labeled samples, pseudo labelling is a very powerful technique that progressively adds more statistically likely labels (pseudo-labels) to the data [Chen et al. \[2020\]](#), [Zou et al. \[2018\]](#). However, it depends on the accuracy of the initial estimate. If our initial estimate of the target label based on VAEGAN is better than other algorithms then it is reasonable to expect that VAEGAN could benefit from pseudo-labeling techniques. Indeed, combining pseudo-labeling techniques and VAEGAN provides a promising direction for future work.

Acknowledgments. This research has been funded by NSF under grants 2134667 “Privacy-Preserving Tiny Machine Learning Edge Analytics to Enable AI-Commons for Secure Manufacturing” and 2112471 “AI Institute for Future Edge Networks and Distributed Intelligence (AI-EDGE).” This research has also been partially sponsored by the U.S. Army Research Laboratory and the U.K. Ministry of Defence under Agreement Number W911NF-16-3-0001. The views and conclusions contained in this document are those of the authors and should not be interpreted as representing the official policies, either expressed or implied, of the U.S. Army Research Laboratory, the U.S. Government, the U.K. Ministry of Defence or the U.K. Government. The U.S. and U.K. Governments are authorized to reproduce and distribute reprints for Government purposes notwithstanding any copyright notation hereon.

References

- Ibrahim Batuhan Akkaya, Fazil Altinel, and Ugur Halici. Self-training guided adversarial domain adaptation for thermal imagery. In *Proceedings of the IEEE/CVF Conference on Computer Vision and Pattern Recognition*, pages 4322–4331, 2021.
- Pablo Arbelaez, Michael Maire, Charless Fowlkes, and Jitendra Malik. Contour detection and hierarchical image segmentation. *IEEE transactions on pattern analysis and machine intelligence*, 33(5):898–916, 2010.
- Konstantinos Bousmalis, George Trigeorgis, Nathan Silberman, Dilip Krishnan, and Dumitru Erhan. Domain separation networks. *Advances in neural information processing systems*, 29, 2016.
- Minghao Chen, Shuai Zhao, Haifeng Liu, and Deng Cai. Adversarial-learned loss for domain adaptation. In *Proceedings of the AAAI conference on artificial intelligence*, volume 34, pages 3521–3528, 2020.
- Jia Deng, Wei Dong, Richard Socher, Li-Jia Li, Kai Li, and Li Fei-Fei. Imagenet: A large-scale hierarchical image database. In *2009 IEEE conference on computer vision and pattern recognition*, pages 248–255. Ieee, 2009.
- Yaroslav Ganin, Evgeniya Ustinova, Hana Ajakan, Pascal Germain, Hugo Larochelle, François Laviolette, Mario Marchand, and Victor Lempitsky. Domain-adversarial training of neural networks. *The journal of machine learning research*, 17(1):2096–2030, 2016.
- Muhammad Ghifary, W Bastiaan Kleijn, Mengjie Zhang, David Balduzzi, and Wen Li. Deep reconstruction-classification networks for unsupervised domain adaptation. In *European conference on computer vision*, pages 597–613. Springer, 2016.
- Ian Goodfellow, Jean Pouget-Abadie, Mehdi Mirza, Bing Xu, David Warde-Farley, Sherjil Ozair, Aaron Courville, and Yoshua Bengio. Generative adversarial networks. *Communications of the ACM*, 63(11):139–144, 2020.
- Kaiming He, Xiangyu Zhang, Shaoqing Ren, and Jian Sun. Deep residual learning for image recognition. In *Proceedings of the IEEE conference on computer vision and pattern recognition*, pages 770–778, 2016.
- Sergey Ioffe and Christian Szegedy. Batch normalization: Accelerating deep network training by reducing internal covariate shift. In *International conference on machine learning*, pages 448–456. PMLR, 2015.

- Yann LeCun, Léon Bottou, Yoshua Bengio, and Patrick Haffner. Gradient-based learning applied to document recognition. *Proceedings of the IEEE*, 86(11):2278–2324, 1998.
- Hong Liu, Mingsheng Long, Jianmin Wang, and Michael Jordan. Transferable adversarial training: A general approach to adapting deep classifiers. In *International Conference on Machine Learning*, pages 4013–4022. PMLR, 2019.
- Xiaofeng Liu, Chaehwa Yoo, Fangxu Xing, Hyejin Oh, Georges El Fakhri, Je-Won Kang, Jonghye Woo, et al. Deep unsupervised domain adaptation: a review of recent advances and perspectives. *APSIPA Transactions on Signal and Information Processing*, 11(1), 2022.
- Yuval Netzer, Tao Wang, Adam Coates, Alessandro Bissacco, Bo Wu, and Andrew Y Ng. Reading digits in natural images with unsupervised feature learning. 2011.
- Kate Saenko, Brian Kulis, Mario Fritz, and Trevor Darrell. Adapting visual category models to new domains. In *Computer Vision–ECCV 2010: 11th European Conference on Computer Vision, Heraklion, Crete, Greece, September 5–11, 2010, Proceedings, Part IV 11*, pages 213–226. Springer, 2010.
- Ankush Singla, Elisa Bertino, and Dinesh Verma. Preparing network intrusion detection deep learning models with minimal data using adversarial domain adaptation. In *Proceedings of the 15th ACM Asia Conference on Computer and Communications Security*, pages 127–140, 2020.
- Eric Tzeng, Judy Hoffman, Kate Saenko, and Trevor Darrell. Adversarial discriminative domain adaptation. In *Proceedings of the IEEE conference on computer vision and pattern recognition*, pages 7167–7176, 2017.
- Mei Wang and Weihong Deng. Deep visual domain adaptation: A survey. *Neurocomputing*, 312: 135–153, 2018.
- Adam Zewe. Avoiding shortcut solutions in artificial intelligence — news.mit.edu. <https://news.mit.edu/2021/shortcut-artificial-intelligence-1102>, 2021. [Accessed 17-May-2023].
- Lei Zhang and Xinbo Gao. Transfer adaptation learning: A decade survey. *IEEE Transactions on Neural Networks and Learning Systems*, 2022.
- Youshan Zhang. A survey of unsupervised domain adaptation for visual recognition. *arXiv preprint arXiv:2112.06745*, 2021.
- Fuzhen Zhuang, Zhiyuan Qi, Keyu Duan, Dongbo Xi, Yongchun Zhu, Hengshu Zhu, Hui Xiong, and Qing He. A comprehensive survey on transfer learning. *Proceedings of the IEEE*, 109(1), 2020.
- Yang Zou, Zhiding Yu, BVK Kumar, and Jinsong Wang. Unsupervised domain adaptation for semantic segmentation via class-balanced self-training. In *Proceedings of the European conference on computer vision (ECCV)*, pages 289–305, 2018.

Appendices

This appendices supply some additional details.

A More Details on Loss Functions

We provide the details of all the loss functions mentioned in Section 3 of the main paper. Recall that the data is given by (x, l, d) where x is the input with x^s and x^t representing the source and target data, respectively. l is the label of the sample, and d is the domain identity.

In unsupervised domain adaptation, the classification loss applies only to the source domain and it is defined as follows:

$$\mathcal{L}_c = - \sum_{i=1}^{N_s} l_i^s \cdot \log \hat{l}_i^s \quad (5)$$

where N_s represents the number of samples from the source domain, l_i^s is the one-hot encoding of the label for the source input x_i^s and \hat{l}_i^s is the softmax output of $C(G(x_i^s))$.

The discriminator loss trains the discriminator to predict whether the DIRep is generated from the source or the target domain. N_t represents the number of samples from target domain and \hat{d}_i is the output of $D(G(x_i))$.

$$\mathcal{L}_d = - \sum_{i=1}^{N_s+N_t} \left\{ d_i \log \hat{d}_i + (1 - d_i) \log (1 - \hat{d}_i) \right\} \quad (6)$$

The generator loss is the GAN loss with inverted domain truth labels:

$$\mathcal{L}_g = - \sum_{i=1}^{N_s+N_t} \left\{ (1 - d_i) \log \hat{d}_i + d_i \log (1 - \hat{d}_i) \right\} \quad (7)$$

For the reconstruction loss, we use the standard mean squared error loss calculated from both domains:

$$\mathcal{L}_r = \sum_i^{N_s} \|x_i^s - \hat{x}_i^s\|_2^2 + \sum_i^{N_t} \|x_i^t - \hat{x}_i^t\|_2^2 \quad (8)$$

where $\hat{x}_i^s = F(G(x_i^s), E(x_i^s))$ and $\hat{x}_i^t = F(G(x_i^t), E(x_i^t))$

Finally, the KL-divergence loss measures the distance between the distribution of DDRep which comes from a Gaussian with mean $\mathbb{E}(DDRep)$ and variance $\mathbb{V}(DDRep)$ and the standard normal distribution.

$$\begin{aligned} \mathcal{L}_{kl} &= D_{KL}(Pr(DDRep) \parallel \mathcal{N}(0, I)) \\ &= -\frac{1}{2}(1 + \log[\mathbb{V}(DDRep)] - \mathbb{V}(DDRep) - \mathbb{E}(DDRep)^2) \end{aligned} \quad (9)$$

B Experiment Details for Fashion-MNIST

B.1 Network architecture

All the methods are trained using the Adam optimizer with the learning rate of $2e - 4$ for 10,000 iterations. We use batches of 128 samples from each domain for a total of 256 samples. When training with our model (VAEGAN), the label prediction pipeline (generator and classifier) has eight fully connected layers (FC1, ..., FC7, FC_OUT). The number of neurons in FC1-4 is 100 for each layer. FC5 is a 100-unit layer that generates DIRep, followed by two 400-unit layers (FC6-7). FC_OUT is the output layer for label prediction. The discriminator and decoder each have four layers with 400 hidden units and followed by the domain prediction layer and reconstruction layer, respectively. The encoder has two layers with 400 units, followed by 1-unit z_{mean} , 1-unit z_{variance} , and 1-unit sampling layer. Each of the 400-unit layers uses a ReLU activation function.

All the other models have the same architecture as VAEGAN when applicable. For the GAN-based approach and DANN, we turn off the decoder and corresponding losses. For the DSN, we keep the same network architecture for common networks and use \mathcal{L}_g for the similarity loss. Furthermore, we implement the shared and private encoders with same shape output vectors [Bousmalis et al. \[2016\]](#).

B.2 Hyperparameters

As suggested in previous work [Ganin et al. \[2016\]](#), the coefficient of the loss, which encourages domain invariant representation, should be initialized as 0 and changed to 1. We use the following schedule for the coefficient of \mathcal{L}_g in all the experiments where t is the training iteration:

$$\lambda = \frac{2}{1 + \exp(-t)} - 1 \quad (10)$$

The increasing coefficient allows the discriminator to be less sensitive to noisy signals at the early stages of the training procedure. For other hyperparameters, we used $\beta = 1, \gamma = \mu = 1$ (the hyperparameters were not tuned using validation samples).

Table 7: Mean classification accuracy (%) of different unsupervised DA approaches for the constructed Fashion-MNIST datasets.

| Model | No cheating | Shift cheating | Random cheating |
|-------------|-------------|----------------|-----------------|
| Source-only | 20.0 | 11.7 | 13.8 |
| GAN-based | 64.7 | 58.2 | 54.8 |
| DANN | 63.7 | 58.0 | 53.6 |
| DSN | 66.8 | 63.6 | 57.1 |
| VAEGAN | 66.9 | 65.7 | 61.6 |
| Target-only | 88.1 | 99.8 | 87.9 |

Table 8: z-test score value comparing VAEGAN to other models for constructed Fashion-MNIST. $z > 2.3$ means the probability of VAEGAN being no better is ≤ 0.01 .

| Model | No cheating | Shift cheating | Random cheating |
|-----------|-------------|----------------|-----------------|
| GAN-based | 1.55 | 3.28 | 3.68 |
| DANN | 2.26 | 4.17 | 4.33 |
| DSN | 0.16 | 2.60 | 3.18 |

We closely follow the setup of weights of the loss functions used in the DSN paper [Bousmalis et al. \[2016\]](#) and DANN paper [Ganin et al. \[2016\]](#). To boost the performance of DSN, we set the coefficient of \mathcal{L}_{recon} to 0.15 and the coefficient of \mathcal{L}_{diff} to 0.05, tuned parameter values determined by [Bousmalis et al. \[2016\]](#) using a validation set of target labels.

B.3 Results and analysis.

Table 7 summarizes the mean classification accuracy of different approaches for three cheating scenarios. In the no cheating scenario, we use the original Fashion-MNIST as source and flip the Fashion-MNIST for the target. We report the z-score of the comparison of the mean classification accuracy of our method with the mean classification accuracy of other methods over five independent runs (see Table 8). The higher the z-score, the more statistical confidence we should have that our method outperforms the other methods. A z-score of 2.33 corresponds to 99% confidence that our method is superior, assuming that the accuracy over different runs will follow a Gaussian distribution.

In the no cheating scenario, VAEGAN outperforms GAN-based and DANN and matches the result of DSN. The performance of GAN-based and DANN results in a 5% accuracy drop for the shift cheating and 10% drop for the random cheating. This validates our concern with the hidden data effect. The source cheating bits can be picked up in the DIREp as they represent an easy solution for the classifier that is trained only with source samples. If that is the case, then the cheating generator would perform poorly for the target domain, which has different cheating bits. Our method has only 1% and 5% accuracy drop respectively and is less vulnerable to the hidden data effect. As a reconstruction-based method, DSN performs better in the presence of cheating bits. In the shift and random cheating, our approach significantly outperforms DSN with a z-score of 2.60 and 3.18 respectively, which shows the correctness of our intuition that penalizing the size of DIREp can result in transferring as much information as possible to the DIREp. In the explicit DIREp algorithm, the DIREp is minimal as it only contains the domain label. Given a richer DIREp, our method leads to a classifier based on the invariant features of the images, which improves its performance on the target data.

C Experiment Details for CIFAR-10

C.1 Network architecture and training procedure

When training with our approach, we implement the network components as deep residual neural networks (ResNets) with short-cut connections [He et al. \[2016\]](#). ResNets are easier to optimize, and sometimes gain accuracy from increased depth. For our approach, we implemented the full-fledged VAEGAN and we added the domain label to the DIREp generated by the encoder. The architecture is shown in Figure 4. The label prediction pipeline is adopted from the ResNet 20 for CIFAR-10 in [He et al. \[2016\]](#). For the generator, the first layer is 3×3 convolutions. Then we use a stack of 6 layers with 3×3 convolutions on the feature maps of size 32. The numbers of filters are 16. The architecture of the classifier consists of a stack of 6×2 layers with 3×3 convolutions on the feature maps of sizes $\{16, 8\}$ respectively. To maintain the network complexity, the number of filters are $\{32, 64\}$. The classifier ends with a global average pooling, and a fully-connected layer with softmax.

For the discriminator, the network inputs are $32 \times 32 \times 16$ domain invariant features. The first layer is 3×3 convolutions. Then we use a stack of 6×3 layers with 3×3 convolutions on the feature maps of sizes 32, 16, and 8 respectively, with 6 layers for each feature map size. The numbers of

Table 9: Averaged classification accuracy (%) of different unsupervised DA approaches for constructed CIFAR-10 dataset with a spectrum of bias.

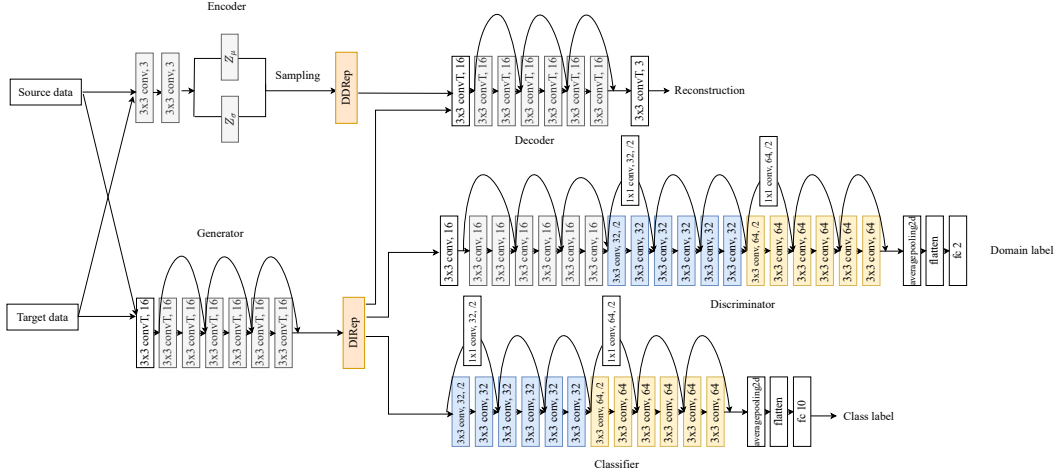


Figure 4: CIFAR10 architecture; inspired by the classical ResNet-20 [He et al. \[2016\]](#)

filters is $\{16, 32, 64\}$ respectively. The discriminator ends with a global average pooling, a 2-way fully-connected layer, and softmax.

The encoder has 4 convolutional layers: three 3×3 filters, two 3×3 filters, two 3×3 filters (z mean) and two 3×3 filters (z variance) respectively. A sampling layer is also implemented which outputs the DDRep from the latent distribution z . The decoder learns to reconstruct an input image by using its DIRep, DDRep and domain bit together. Hence, the inputs of the decoder are $32 \times 32 \times 19$ concatenated representations. The configuration of the decoder is the inverse of that of the generator.

We implemented the same ResNet-based architecture for all other approaches (when applicable). We use a weight decay of 0.0001 and adopt the BN [Ioffe and Szegedy \[2015\]](#) for all the experiments. The hyperparameters are the same as the ones in Section B.2.

C.2 Results and analysis

We report the mean accuracy of different unsupervised DA methods and our approach on the target test set in Table 9. The z-scores of comparing our method with other methods are shown in Table 10.

For all the DA tasks with varying biases, we observe that our approach outperforms the other approaches in terms of accuracy in the target set. This improvement is most pronounced when the source set has 60% and 80% bias levels, which means that over half of the source data has a spurious correlation between their color planes and labels. The poor performance of the GAN-based and DANN approaches is another example where the generator in these approaches learns a DIRep that depends on the spurious correlation. This false representation leads to an issue similar to over-fitting where the model performs well on the source data, but does not generalize well on the target data in which the same correlation does not exist. In the DSN approach, the shared representation contains some domain-independent information other than the cheating clues which helps classification in the target domain. However, it does not directly address the problem of making the domain invariant representation richer for classification. We postulate that the inferior performance of the DSN approach

Table 10: z-test score value comparing VAEGAN to other models for constructed CIFAR-10. $z > 2.3$ means the probability of VAEGAN being no better than the other models is ≤ 0.01 .

| Model | 0% bias | 20% bias | 40% bias | 60% bias | 80% bias | 90% bias | 100% bias |
|-----------|---------|----------|----------|----------|----------|----------|-----------|
| GAN-based | 5.23 | 3.20 | 5.93 | 12.8 | 11.31 | 7.20 | 4.58 |
| DANN | 5.44 | 3.42 | 6.22 | 13.2 | 12.02 | 7.79 | 5.70 |
| DSN | 2.68 | 3.00 | 3.95 | 3.47 | 7.43 | 3.78 | 2.23 |

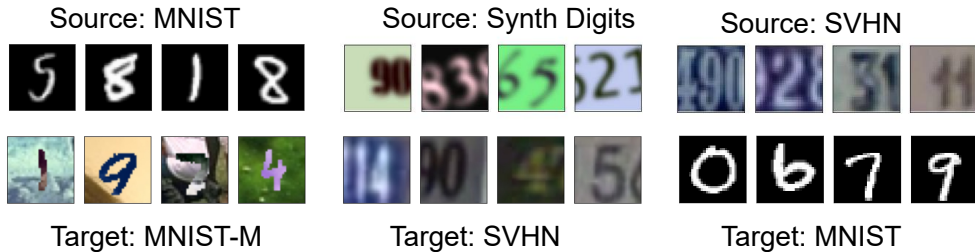


Figure 5: Example images from four domain adaptation benchmark datasets for three scenarios.

may stem from the way its shared and private representations are trained. The difference loss in DSN only encourages orthogonality between the shared and the private representations in a linear way, which can be less effective in separating domain dependent and independent information for difficult DA scenarios.

D SVHN, MNIST, MNIST-M and Synth Digits

We evaluate the empirical performance of VAEGAN on four widely used domain adaptation benchmarks: MNIST [LeCun et al. \[1998\]](#), MNIST-M [Ganin et al. \[2016\]](#), Street View House Number [Netzer et al. \[2011\]](#) and synthetic digits [Ganin et al. \[2016\]](#). We use three unsupervised domain adaptation pairs: 1) MNIST \rightarrow MNIST-M, 2) Synth Digits \rightarrow SVHN, and 3) SVHN \rightarrow MNIST. Example images from all four datasets are provided in Figure 5. We implement our CNN topology based on the ones used in [Bousmalis et al. \[2016\]](#) and [Ganin et al. \[2016\]](#). We used Adam with the learning rate of 0.0002 for 25,000 iterations. The batch size is 128 for each domain. We did not use validation samples to tune hyperparameters. To make fair comparisons, we follow the instructions in [Bousmalis et al. \[2016\]](#) and activate the \mathcal{L}_g after 20,000 steps of training. For other hyperparameters, we used $\beta = 1$, $\gamma = 1$, and $\mu = 1$.

Note, that none of these data sets contain information correlated with the label that is available in the source but not the target, because of the way they were constructed. Our techniques are particularly applicable when there is a superfluous or shortcut means to classify in the source, so we don't have an advantage we have in many more natural settings. Never the less our techniques are at least competitive.

MNIST to MNIST-M. We use the MNIST dataset as the source domain, and a variation of MNIST called MNIST-M as the target. MNIST-M was created by blending digits from the original MNIST set over patches randomly extracted from color photos from BSDS500 [Arbelaez et al. \[2010\]](#).

Synthetic Digits to SVHN. This scenario is widely used to demonstrate the effectiveness of the algorithm when training on synthetic data and testing on real data. We use synthetic digits as the source and Street-View House Number data set SVHN as the target.

SVHN to MNIST. In this experiment, we further increase the gap between the two domains. The digit shapes in SVHN are quite distinct from those handwritten digits in MNIST. Furthermore, SVHN contains significant image noise, such as multiple digits in one image and blurry background.

Results Table 11 shows the results on the digits datasets. We cited the results from each study to make a fair comparison. GAN-based method is omitted from the table since the paper does not

Table 11: Mean classification accuracy (%) of different unsupervised domain adaptation approaches for widely used benchmarks. The results are cited from each study. When we attempted to replicate the DSN results we only achieved 80.0% not 83.2% and that 80.0% may be more comparable to the 81.0% for VAEGAN.

| Model | MNIST to MNIST-M | Synth Digits to SVHN | SVHN to MNIST |
|-------------|---------------------|-------------------------|------------------|
| Source-only | 56.6 | 86.7 | 59.2 |
| DANN | 76.6 | 91.0 | 73.8 |
| DSN | 83.2 | 91.2 | 82.7 |
| VAEGAN | 81.0 | 91.1 | 85.8 |
| Target-only | 98.7 | 92.4 | 99.5 |

Table 12: Mean classification accuracy (%) of different unsupervised domain adaptation approaches for the office dataset. We have cited the original results (if applicable) and in parentheses we show the results reported in [Chen et al. \[2020\]](#) with data augmentation.

| Model | $A \rightarrow W$ | $D \rightarrow A$ | $W \rightarrow A$ |
|-------------|--------------------|-------------------|-------------------|
| Source-only | 64.2 (68.4) | - (62.5) | - (60.7) |
| DANN | 73.0 (82.0) | - (68.2) | - (67.4) |
| ADDA | 75.1 (86.2) | - (69.5) | - (68.9) |
| VAEGAN | 82.0 | 72.9 | 72.0 |

test on digit datasets. In MNIST \rightarrow MNIST-M and Synth Digits \rightarrow SVHN, we were not able to achieve the published results for DSN. The previously published results for DSN were based on using hyperparameters chosen after using 1000 labeled samples from the target. Our parameters were chosen without use of target labels. In summary, VAEGAN outperforms DSN on the difficult SVHN \rightarrow MNIST shift and achieves comparable results on the Synth Digits \rightarrow SVHN shift.

E Office dataset

Our method was evaluated on the Office dataset, which comprises three distinct domains: Amazon, DSLR, and Webcam. Unlike larger datasets, the Office dataset is relatively small, containing only 2817 labeled images across 31 different categories in the largest domain. Due to the limited data availability, we opted to utilize the ResNet-50 architecture pretrained on the ImageNet dataset, following a common approach in recent domain adaptation studies [Tzeng et al. \[2017\]](#), [Chen et al. \[2020\]](#). This choice allowed us to leverage the knowledge gained from ImageNet’s large-scale dataset and apply it to our specific domain adaptation task. By employing the same network architecture as [Tzeng et al. \[2017\]](#), we ensured a fair and direct comparison of our method’s performance, particularly in the challenging $D \rightarrow A$ and $W \rightarrow A$ scenarios where the source training data is limited (see Table 12). We include the original results from the DANN and ADDA papers as well as the new results from [Chen et al. \[2020\]](#) with training data augmentation. We follow the training protocol in DANN and ADDA when training VAEGAN which does not use any data augmentation techniques.